

Antisense *COOLAIR* mediates the coordinated switching of chromatin states at *FLC* during vernalization

Tibor Csorba^{1,2}, Julia I. Questa¹, Qianwen Sun^{1,3}, and Caroline Dean⁴

Department of Cell and Developmental Biology, John Innes Centre, Norwich NR4 7UH, United Kingdom

Contributed by Caroline Dean, October 5, 2014 (sent for review July 10, 2014; reviewed by Justin Goodrich and Leonie Ringrose)

Long noncoding RNAs (lncRNAs) have been proposed to play important roles in gene regulation. However, their importance in epigenetic silencing and how specificity is determined remain controversial. We have investigated the cold-induced epigenetic switching mechanism involved in the silencing of *Arabidopsis thaliana* FLOWERING LOCUS C (*FLC*), which occurs during vernalization. Antisense transcripts, collectively named *COOLAIR*, are induced by prolonged cold before the major accumulation of histone 3 lysine 27 trimethylation (H3K27me3), characteristic of Polycomb silencing. We have found that *COOLAIR* is physically associated with the *FLC* locus and accelerates transcriptional shutdown of *FLC* during cold exposure. Removal of *COOLAIR* disrupted the synchronized replacement of H3K36 methylation with H3K27me3 at the intragenic *FLC* nucleation site during the cold. Consistently, genetic analysis showed *COOLAIR* and Polycomb complexes work independently in the cold-dependent silencing of *FLC*. Our data reveal a role for lncRNA in the coordinated switching of chromatin states that occurs during epigenetic regulation.

flowering | long noncoding RNA | histone modifications | Polycomb | *Arabidopsis*

An important developmental transition in plants is the switch from vegetative growth to flowering. Several pathways that control flowering converge to regulate expression of the gene encoding the floral repressor FLOWERING LOCUS C (*FLC*) (1, 2). Vernalization, the quantitative acceleration of flowering by prolonged cold, leads to the epigenetic silencing of *FLC* (1, 3). Polycomb Repressive Complex 2 (PRC2) is required for vernalization (4) with the core PRC2 recruited to the *FLC* locus before silencing. Cold exposure induces formation of a modified PRC2, PHD-PRC2 involving the Plant Homeodomain (PHD) proteins (VRN5 and VIN3), at an intragenic nucleation site (5). Upon return to warm conditions, PHD-PRC2 spreads across the whole *FLC* locus, resulting in high levels of histone 3 lysine 27 trimethylation (H3K27me3) and stable epigenetic repression. The quantitative nature of vernalization was found to be the result of a cell autonomous switch between bistable epigenetic states (6). The silent state, which is reflected by H3K27me3 accumulation and increasing cold, progressively increases the proportion of cells in which this switch has occurred. A detailed temporal and spatial analysis exploring the opposing expression state showed H3K36me3 is the most likely modification with an antagonistic role to H3K27me3 (7). However, the lack of an absolute mirror profile between H3K27me3 and H3K36me3 at *FLC* suggests additional factors are necessary for epigenetic switching at *FLC* (7).

COOLAIR, a group of long antisense RNAs expressed from the *FLC* locus, has an important role in mediating *FLC* expression in nonvernalized plants (8–10). *COOLAIR* is alternatively spliced and alternatively polyadenylated with two major classes in the warm, the proximally polyadenylated class I and the distally polyadenylated class II (Fig. 1 *A* and *B* and refs. 11 and 12). Increased proximal polyadenylation enhances H3K4me2 demethylase activity and reduces *FLC* transcription,

resulting in a positive feedback mechanism that reinforces proximal polyadenylation and low expression of *FLC* (9, 10). Distal polyadenylation is associated with a high expression state of the locus, but it is still unclear whether use of the distal site causes, or is a consequence of, increased *FLC* transcription (9, 12). In addition to this processing of the *COOLAIR* transcript, the *COOLAIR* promoter is regulated by the presence of an R loop (13). Stabilization of the R loop by the homeodomain protein NDX1 reduces *COOLAIR* transcription (13). *COOLAIR* transcription is also regulated by cold, with a transient expression peak after 2–3 wk of cold exposure (11). Addition of *COOLAIR* promoter sequences as the 3' terminator of a GFP sensor construct was sufficient for cold-induced reduction of GFP expression. However, the role of *COOLAIR* in the cold-mediated epigenetic silencing during vernalization remained unclear because plants carrying insertions into the *COOLAIR* promoter that attenuate *COOLAIR* expression were found to vernalize (14).

Here, we have sought to clarify the role of *COOLAIR* in vernalization by analyzing an *FLC* gene carrying a replacement 3' region, so lacking the *COOLAIR* promoter. We show that *COOLAIR* significantly accelerates *FLC* transcriptional repression in the cold. *COOLAIR* RNA was found to physically

Significance

Long noncoding RNAs (lncRNAs) play important roles in chromatin regulation in higher eukaryotes. Studies analysing how lncRNAs influence Polycomb silencing suggested they specifically bind and recruit Polycomb Repressive Complex 2 (PRC2) to defined targets. However, the promiscuous binding of PRC2 to RNA has raised questions as to the mechanism by which lncRNA contributes to Polycomb silencing. We investigate the function of a set of cold-induced antisense transcripts in the Polycomb-dependent epigenetic silencing of a floral repressor gene in *Arabidopsis*. Through analysis of a transgene, in which antisense transcripts are no longer cold-induced, we show that these antisense transcripts are required for coordinated switching of opposing chromatin states. This mechanism links transcriptional shutdown by cold to long-term epigenetic silencing.

Author contributions: T.C., J.I.Q., Q.S., and C.D. designed research; T.C., J.I.Q., and Q.S. performed research; T.C., J.I.Q., Q.S., and C.D. analyzed data; and T.C., J.I.Q., Q.S., and C.D. wrote the paper.

Reviewers: J.G., University of Edinburgh; and L.R., Institute of Molecular Biotechnology GmbH.

The authors declare no conflict of interest.

Freely available online through the PNAS open access option.

¹T.C., J.I.Q., and Q.S. contributed equally to this work.

²Present address: National Agricultural Research and Innovation Centre, Gödöllő, 2100, Hungary.

³Present address: Center for Plant Biology, School of Life Sciences, Tsinghua University, and Tsinghua-Peking Center for Life Sciences, Beijing 100084, China.

⁴To whom correspondence should be addressed. Email: caroline.dean@jic.ac.uk.

This article contains supporting information online at www.pnas.org/lookup/suppl/doi:10.1073/pnas.1419030111/-DCSupplemental.

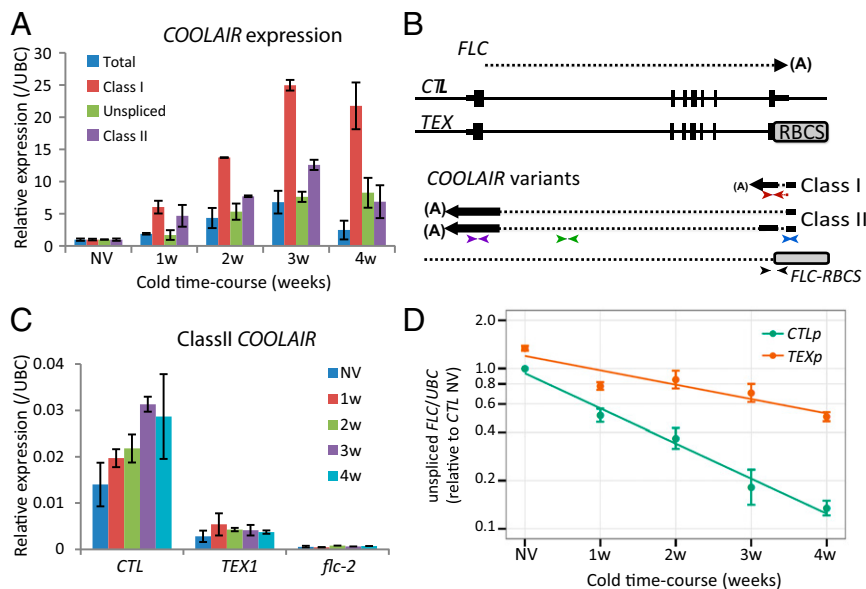


Fig. 1. *COOLAIR* accelerates *FLC* transcriptional down-regulation during vernalization. (A) Quantitative RT-PCR (qRT-PCR) analysis showing *COOLAIR* forms are differentially induced during a time-course of cold exposure, nonvernalized material (NV), 1 wk cold exposure (1w), 2 wk cold (2w), 3 wk cold (3w), and 4 wk cold (4w). Values are normalized to NV (set as 1), means \pm SEM of three biological replicates. (B) Schematic representation of the *FLC* genomic locus and sense and antisense RNA transcripts in the control (*CTL*) and Terminator EXchange lines (*TEX*). *CTL* lines were generated by transformation of *FLC* genomic construct (15 kb of the *FLC* locus, *FLC-15*) into *flc-2* FRI background. *TEX* lines were generated as described (9, 10). For antisense transcripts in *TEX* lines, a combination of *FLC* and *RBCS* primers were used. (A), pA sites; *RBCS*, Rubisco gene terminator. The position of the primers used in qRT-PCR analysis to assess class I (red arrows), class II (purple arrows), unspliced antisense (green arrows), total *COOLAIR* (blue arrows), or antisense RNA transcript derived from *TEX* construct (black arrows) are shown; sequences are listed in *SI Appendix, Table S2*. (C) qRT-PCR analysis of class II *COOLAIR* relative to UBC in *CTL* and *TEX*. Values are means \pm SEM of three biological replicates. (D) Down-regulation of *FLC* unspliced RNA is significantly abrogated ($P < 0.005$) in *TEX* compared with control during cold exposure. *CTLp* and *TEXp* correspond to a mix of 50 T3 transgenic lines (*Materials and Methods*). Values are means \pm SEM of five biological replicates and are plotted on a log scale. NV levels are also significantly different ($P < 0.001$).

associate with *FLC* chromatin in two important regulatory regions. Disruption of *COOLAIR* expression prevented the cold-induced reduction of H3K36 methylation, without changing the H3K27me3 accumulation dynamics, at the intragenic *FLC* nucleation site. This work reveals a role for *COOLAIR* in the coordinated switching of chromatin states that occurs during cold, linking transcriptional shutdown with epigenetic silencing.

Results

***COOLAIR* Isoforms Accumulate Differentially in the Cold.** To further understand roles of *COOLAIR*, we first undertook a thorough analysis of the accumulation of *COOLAIR* isoforms over a time course of cold exposure (Fig. 1A). The unspliced, class I and class II isoforms of *COOLAIR* all accumulated during cold with, in this experimental setup, a maximum induction at 3 wk cold. However, induction of the class I isoform was several fold higher than the others, consistent with proximal polyadenylation correlating with reduced levels of *FLC* transcription. To distinguish whether the accumulation in the cold was due to transcriptional induction or higher transcript stability in the cold, we measured *COOLAIR* steady-state levels in the presence of cordycepin, a chain termination adenosine analog (3'-deoxyadenosine) (15). The half-life of the *COOLAIR* transcript increased slightly in the cold ($t_{1/2}^{NV} = 100$ min, $t_{1/2}^{2w} = 240$ min; *SI Appendix, Fig. S1A*), but this change only partly explained the robust increase (seven- to eightfold) in *COOLAIR* RNA levels (Fig. 1A). Accumulation of *COOLAIR* during cold is therefore a consequence of both transcript stabilization and transcriptional induction.

***COOLAIR* Accelerates Transcriptional Shutdown of *FLC* During Cold Exposure.** To investigate the biological functions of *COOLAIR* in *FLC* regulation, we had generated plant lines impaired in *FLC* antisense transcription by exchanging the *FLC* terminator/*COOLAIR*

promoter with the strong *RBCS* terminator (*RBCS3B* At5G38410) in the *flc-2* background to form Terminator EXchange lines, *TEX* (9, 10) (Fig. 1B). *flc-2* is a loss-of-function *FLC* genotype, which has a deletion/rearrangement within the endogenous *FLC* gene (1). The *TEX* lines were compared with transgenic plant lines carrying an intact *FLC* gene (control line, *CTL*; ref. 16) (Fig. 1B). Because expression of transgenes vary depending on the genomic context of their integration, the analysis was carried out both on selected representative lines (*CTL* and *TEX1*) or a pool of 50 individual T3 lines (referred as *CTLp* and *TEXp*). First, we confirmed that the level of *COOLAIR* transcription in *TEX* lines is lower than wild-type and is not cold inducible (Fig. 1C and *SI Appendix, Fig. S2 A–C* and *S3 A and C*). Next, we assessed the effect of *COOLAIR* disruption on *FLC* transcription by measuring the level of *FLC* unspliced transcript in *TEX* samples. Transcription of *FLC* is significantly higher in nonvernalized plants (pooled samples, Fig. 1D) and is reduced by cold exposure much more slowly compared with lines carrying an intact *FLC* expressing *COOLAIR* (Fig. 1D, and in single line *SI Appendix, Fig. S3B*). To analyze how *COOLAIR* exerts this effect, we compared *FLC* unspliced transcript stability in *TEX1* versus *CTL* line. No significant differences in *FLC* half-life were detected ($t_{1/2}^{CTL} = 72$ min, $t_{1/2}^{TEX1} = 88$ min; *SI Appendix, Fig. S1D*). The difference in the amount of unspliced *FLC* transcript levels between the *TEX* and *CTL* lines therefore is likely to be the consequence of increased *COOLAIR* transcriptional activity.

The *FLC* mRNA (fully spliced) levels did not closely follow the dynamics of the unspliced *FLC* RNA during cold exposure, with almost no decrease in *FLC* mRNA for the first 2 wk of cold exposure (*SI Appendix, Fig. S2D*). These results suggest that *FLC* mRNA has a long half-life of many days that is not significantly affected by cold exposure (*SI Appendix, Fig. S1C*). The multiple stability motifs (17) found in the 3' UTR of *FLC* may contribute

to this long half-life (*SI Appendix*, Fig. S1F). The *FLC-TEX* transcript (missing the *FLC* 3' UTR) was found to be slightly less stable (*SI Appendix*, Fig. S1E). The higher levels of *FLC-TEX* in both before and during vernalization are thus likely due to increased transcription, reinforcing the view that *COOLAIR* accelerates transcriptional shutdown of *FLC* during cold exposure.

COOLAIR Associates with FLC Genomic DNA. We have shown that *COOLAIR* up-regulation does not depend on *FLC* sense transcriptional down-regulation (11). However, if sense and antisense transcription occur simultaneously at the same locus, increased antisense transcription could function to transcriptionally interfere with sense transcription. With this question in mind, we compared data from custom tiling arrays that contained both strands of the entire *FLC* genomic region at single nucleotide resolution (*SI Appendix*, Fig. S4, see also ref. 11). The arrays had been hybridized with RNA from both warm and 2-wk cold-treated plants. There was no indication that *COOLAIR* transcription caused transcriptional interference with *FLC* transcription, i.e., that *FLC* unspliced transcripts were more abundant at the 5' end of the gene as *COOLAIR* transcription increased (*SI Appendix*, Fig. S4). In the absence of data supporting a transcriptional interference mechanism, we searched for other mechanisms. Many lncRNAs have been shown to localize to nuclei and induce chromatin changes on their target genes (18). We therefore checked the subcellular localization of *COOLAIR* and found that whereas spliced forms are efficiently exported, both spliced and unspliced *COOLAIR* were found in nuclear fractions (*SI Appendix*, Fig. S5). To address whether *COOLAIR* has ON-chromatin roles, Chromatin Isolation by RNA Purification (ChIRP) was performed (Fig. 2 and *SI Appendix*, Figs. S6 and S7; ref. 19). *COOLAIR* RNA but not *UBC* RNA was efficiently precipitated by using biotinylated antisense DNA oligo probes (the location of the DNA probes are shown on Fig. 2; sequences listed in *SI Appendix*, Table S1) and consistent with its induction by cold, higher amounts of *COOLAIR* RNA could be precipitated from cold-treated samples (*SI Appendix*, Fig. S7 A–C). Sequencing of the coprecipitated DNA showed *COOLAIR* enriched over the whole *FLC* locus (*SI Appendix*, Fig. S6) but concentrated in two discrete regions of the *FLC* genomic DNA, the nucleation region and the 3' region of the gene/*COOLAIR* promoter (Fig. 2 and PCR validation in *SI Appendix*, Fig. S7D). These regions are colinear with *COOLAIR* exon locations but not to the biotin oligo locations used in the ChIRP (Fig. 2). The DNA signal was reduced when samples were pretreated with RNaseA/H, differentially affected by proteinase K (*SI Appendix*, Fig. S7D) and was completely abolished when glutaraldehyde cross-linking was omitted. This result suggests the

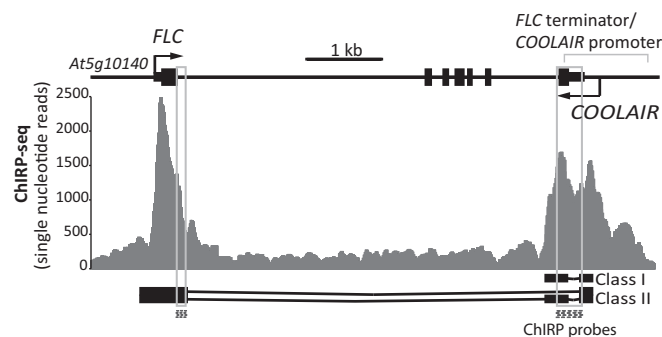


Fig. 2. *COOLAIR* associates *in cis* with *FLC* chromatin. ChIRP deep sequencing analysis data shows *COOLAIR* associates with *FLC* chromatin in two distinct regions. Locations of biotinylated DNA probes used for *COOLAIR* ChIRP are shown (dashed boxes). A schematic of the *FLC* locus is shown with the structure of the class I and class II *COOLAIR* transcripts.

different *COOLAIR*/DNA interactions have different requirements for protein factors. When we analyzed the amount of associated DNA that copurified with *COOLAIR* in nonvernalized and 2-wk cold-treated samples, only a minor difference was observed. We conclude therefore that most of *COOLAIR* induced in cold is in the OFF-chromatin fraction. The genomic locations of the ON-chromatin *COOLAIR* have both been implicated as important for *FLC* regulation. The nucleation region is where the localized increase of H3K27me3 and parallel decrease of H3K36me3 occurs (6, 7). The 3' region of the gene/*COOLAIR* promoter has been shown to contain an R-loop that suppresses *COOLAIR* transcription (13). This region also shows dynamic changes in histone modifications during vernalization (7), suggesting that *COOLAIR* might facilitate chromatin modification of *FLC* chromatin.

COOLAIR Effect on FLC Transcriptional Shutdown During Vernalization Is Independent of Polycomb Machinery and H3K27me3 Accumulation.

Cold exposure gradually increases H3K27me3 accumulation at the nucleation site within the *FLC* gene through the activity of the PHD-PRC2 complex (5, 20). Upon return to warm, a modified PHD-PRC2 and H3K27me3 spread to cover the length of the *FLC* locus (6). To test the role of *COOLAIR* in these changes, we compared H3K27me3 levels at *FLC* in *TEX* compared with control lines (Fig. 3 A and B). No significant differences could be observed in the nucleation of H3K27me3 at *FLC* during vernalization (Fig. 3 A and B). This data suggests that *COOLAIR* is not essential for the deposition of the H3K27me3 modification.

We also asked whether nascent RNAs derived from *FLC* could interact with the PHD-PRC2 complex. RNA-immunoprecipitation (RIP) experiments using GFP-tagged VERNALIZATION 5 (VRN5) and SWINGER (SWN) (21) were undertaken. No enrichment with sense or antisense RNA originating from *FLC* was found (*SI Appendix*, Fig. S8 A–F). Based on the ChIP and RIP data, we conclude that *COOLAIR* does not accelerate the reduction in *FLC* transcription during vernalization by targeting PRC2-PHD or modifying its H3K27me3 activity.

COOLAIR Mediates Reduction in H3K36me3 at FLC. We have recently shown that for many phases of the vernalization process, H3K36me3 and H3K27me3 show opposing profiles in the *FLC* nucleation region (7). H3K36me3 and H3K27me3 were found to rarely coexist on the same histone tail, an antagonism that was shown to be functionally important (7). We therefore compared H3K36me3 levels at *FLC* between *CTL* and *TEX* lines. H3K36me3 levels were higher in the nucleation region before cold and did not decrease during the 4 wk of cold exposure in the *TEX* lines (Fig. 3D), in contrast to *CTL* where levels decreased over the 4-wk cold exposure (Fig. 3C). Whereas H3K27me3 accumulation occurred normally in the *TEX* lines, the removal of *COOLAIR* disrupted the coordinated changes in H3K27me3/H3K36me3 at the nucleation region. H3K4me3 levels often parallel H3K36me3 so we also analyzed H3K4me3 dynamics in *CTL* and *TEX* lines. Removal of *COOLAIR* also disrupted cold-induced reduction of H3K4me3 levels in the nucleation region (*SI Appendix*, Fig. S9).

H3K36me3 and H3K27me3 Can Be Modulated Independently in FLC Silencing.

Interestingly, the high levels of H3K36me3 at the nucleation region in the *TEX* lines did not limit accumulation of H3K27me3 modifications (Fig. 3 B and D). Mutually exclusive histone modification states are predicted to result from linked positive feedback mechanisms connecting production of one modification with removal of the opposing one (22). The ability to disconnect the changes in H3K36me3 and H3K27me3 in the *TEX* lines suggests that their opposing profiles result from coordinated, but not obligatory, linked methylation/demethylation processes.

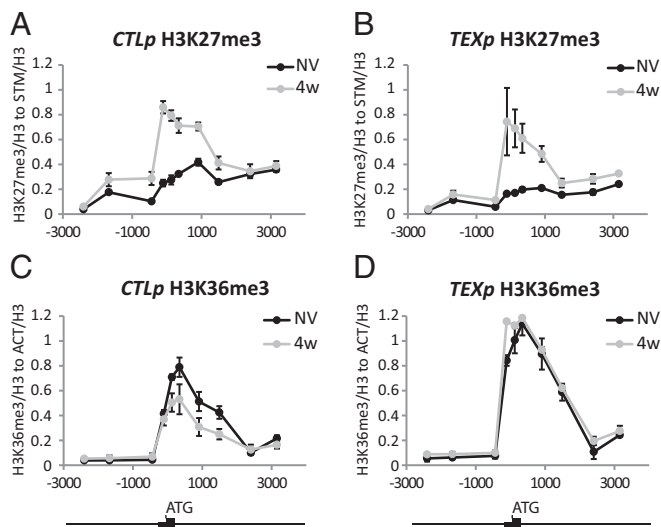


Fig. 3. *COOLAIR* differentially affects the dynamics of H3K36me3 and H3K27me3 during cold-induced silencing at *FLC*. ChIP analysis of H3K27me3 in control lines (A) and *TEX* lines (B). ChIP analysis of H3K36me3 in control lines (C) and *TEX* lines (D). Nonvernalized (NV) and 4 wk vernalized (4w) samples were compared. Small and big boxes on the schematic below show the *FLC* 5' UTR and exon 1, respectively. Numbers define positions from translation start site (ATG). Values are means \pm SEM of three biological replicates.

To further understand these connections we exploited *vm5*, a mutation in a component of the PRC2–PHD complex (23). In *vm5*, H3K27 methylation is impaired, so H3K27me3 levels at *FLC* remain low during vernalization (Fig. 4 A and C). Consequently, levels of unspliced *FLC* (Fig. 5A) and spliced variants of *COOLAIR* are elevated because of a higher transcriptional activity in the absence of Polycomb-mediated repression (SI Appendix, Fig. S10). *vm5*, however, did not affect the dynamics of cold induction of *COOLAIR* (SI Appendix, Fig. S10). Although H3K27 methylation is impaired, H3K36me3 reduction during cold was not affected by *vm5* (Fig. 4 B and D). These data indicate that removal of H3K36me3 during vernalization is not a direct consequence of H3K27me3. Because the *TEX* transgene is affected in H3K36me3 removal but not H3K27me3 deposition (Fig. 3 A–D), the H3K36me3 and H3K27me3 changes are likely to be coordinated processes linking transcriptional shutdown with epigenetic silencing. We predicted that the *vm5* mutation would have a dominant effect on H3K27me3 modification in a *vm5/TEX* genotype. Similarly, *TEX* modification would be dominant in defining H3K36me3 in *vm5/TEX* during cold. The pattern of chromatin modifications in *vm5/TEX* behaved as predicted (Fig. 4 E and F), reinforcing the view that reduction in H3K36me3 and increase in H3K27me3 act in parallel to regulate *FLC* silencing. We tested the consequence of disrupting both processes on the transcriptional down-regulation of *FLC* during vernalization. Reduction of *FLC* transcription, as assayed by unspliced transcript levels, occurred more slowly in *vm5* and in *TEX* compared with wild-type and control lines, but was completely abolished in the *vm5/TEX* double mutant (Fig. 5 A and B). *FLC* down-regulation and silencing in the cold is therefore a consequence of parallel activities that result in H3K27 trimethylation and H3K36me3 demethylation (Fig. 5C).

Discussion

We have investigated the role of the antisense *COOLAIR* in the epigenetic silencing mechanism underlying vernalization by analyzing an *FLC* gene lacking the *COOLAIR* promoter. We found that *COOLAIR* plays a major role during the cold accelerating *FLC* transcriptional repression in a mechanism involving

reduction of H3K36 methylation. This mechanism functions in parallel to the Polycomb processes that result in accumulation of H3K27me3 at the intragenic *FLC* nucleation site. *COOLAIR* is thus important in the coordinated switching of chromatin states that occurs during cold, linking transcriptional shutdown with epigenetic silencing. How could *COOLAIR* lead to reduction in H3K36me3? *COOLAIR* RNA itself, as an ON-chromatin or OFF-chromatin fraction, may be responsible for H3K36me3 demethylation. This function could be achieved through a positive effect on a demethylase (by directing remodeling complexes) or due to a negative effect on a methyltransferase (inhibition of activity, obstruction of its binding by the ON-chromatin fraction, or by a decoy effect of the OFF-chromatin fraction). Candidate *COOLAIR* interacting H3K36 methyltransferase enzymes could be EARLY FLOWERING IN SHORT DAYS (EFS) (24, 25), AtPAF1c-mutant VIP4 methyltransferase (26), or Ash1 homologs. Reports have shown that the conserved Trithorax group protein Ash1 is an H3K36-specific dimethylase (27, 28). In *Arabidopsis*, the Ash1 homolog SDG4 was shown to methylate H3K4 and H3K36 (29). Another Ash1 homolog, SDG8, was shown to contribute to flowering time regulation through changed H3K36 methylation at *FLC* (30). Although H3K36 demethylase are known in animal systems (31), their identification in *A. thaliana* will be necessary to test potential positive effects of *COOLAIR* on their activity.

Association of *COOLAIR* at the *FLC* chromatin, as evidenced by the ChIRP experiments, might influence association of chromatin complexes with the *FLC* nucleation site. The RNA-IP experiments showed no specific association of *COOLAIR* with the PHD–PRC2 complex (SI Appendix, Fig. S8). However, these type of analyses need to be undertaken with the appropriate H3K36 methyltransferases and demethylases. How lncRNAs generally lead to chromatin complex activity in specific chromosomal domains is unclear (32). An influence on

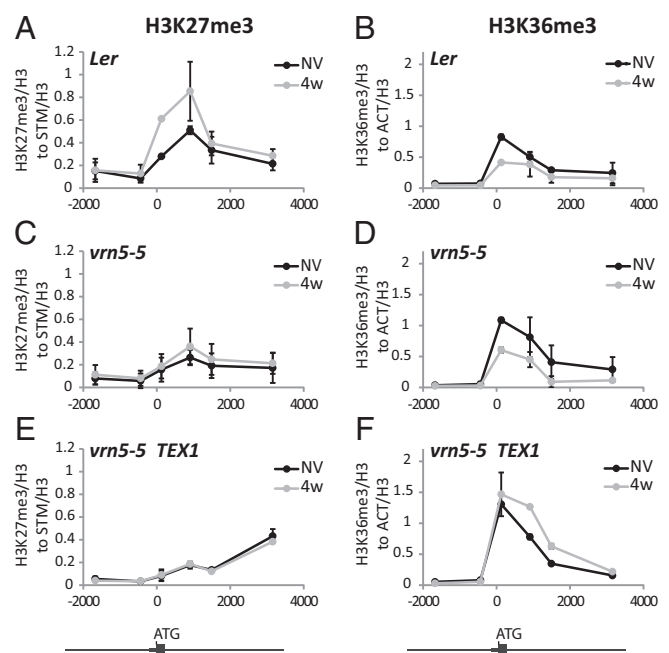


Fig. 4. H3K36me3 and H3K27me3 change independently of each other. ChIP showing H3K27me3 dynamics in Landsberg *erecta* (Ler) (A), *vm5-5* (C), and *vm5-5/TEX1* plants (E), nonvernalized (NV), after 4 wk cold (4w). ChIP showing H3K36me3 dynamics in Ler (B), *vm5-5* (D), and *vm5-5/TEX1* plants (F) nonvernalized (NV), after 4 wk cold (4w). Numbers define positions from translation start site (ATG). Values are means \pm SEM of three biological replicates.

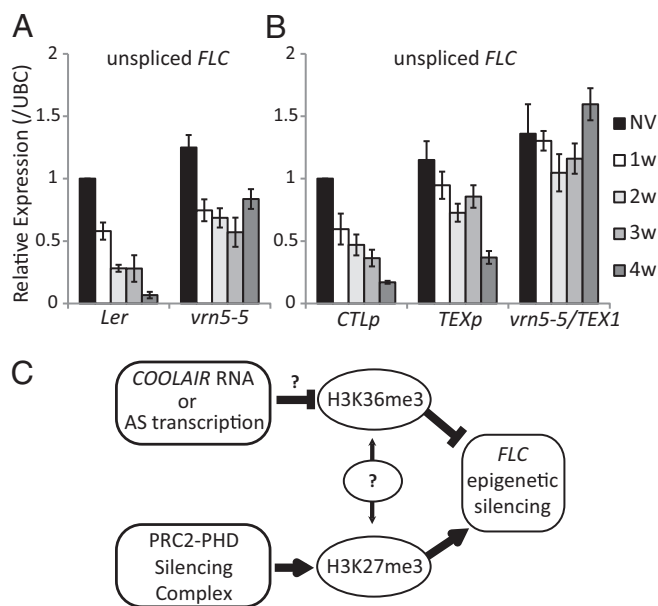


Fig. 5. Loss of cold-induced transcriptional repression of *FLC* is additive when *vrn5* is combined with a *TEX* transgene. qRT-PCR analysis of unspliced *FLC* RNA through a time-course of cold exposure in *Ler* and *vrn5-5* plants (A) and *CTL*, *TEX* lines or *vrn5-5/TEX1* (B). Values are means \pm SEM of three biological replicates. (C) Proposed model: *COOLAIR* negatively affects H3K36me3-methylation status and functions independently of PHD-PRC2-mediated H3K27 trimethylation to promote *FLC* silencing during vernalization.

local association/dissociation rates of chromatin complexes to their respective modifications may be an important contributing factor (33).

Our finding that the opposing profiles of H3K27me3 and H3K36me3 during vernalization can be disconnected has important implications in understanding epigenetic switching mechanisms. Bistable epigenetic states are thought to arise from positive feedback, reinforcing mutually exclusive histone modifications (22). The ability to disconnect the changes in H3K36me3 and H3K27me3 in the *TEX* lines suggests that their opposing profiles result from coordinated, but not obligatory linked, *COOLAIR*-PHD-PRC2 activities. Separately, modifying the generation of active and repressive histone modifications may provide a “fail-safe” mechanism where each one reinforces the other. In *vrn5* or *TEX*, where only one of the pathways is faulty, *FLC* transcriptional silencing still occurs, just at a slower rate, whereas in the *vrn5/TEX*, it is completely abolished. How exactly these two modification systems are integrated with each other remains an open question (Fig. 5C).

An apparently contradictory answer with respect to the importance of *COOLAIR* in vernalization has been found through the analysis of *Arabidopsis* plants containing T-DNA insertions in the *COOLAIR* promoter, or *FLC* gene modules missing the 3' end region (14, 34). Vernalization was found to still accelerate flowering in these plants, although in one of the T-DNA lines (SALK_140021), *FLC* transcriptional repression was slower (14). In fact, we also find that after >4 wk cold regimes, *FLC* silencing is reasonably advanced in the *TEX* lines and sufficient for early flowering to occur when the plants are returned to the warm (SI Appendix, Fig. S11). One complication in this comparison, however, is that flowering time may be affected by the slightly shorter

half-life of the *FLC-TEX* transcript compared with the *FLC* transcript (SI Appendix, Fig. S1E) or an altered polyadenylation of the *FLC-TEX* mRNA. However, we would still conclude that *COOLAIR* RNA or transcription is not absolutely essential for vernalization in laboratory vernalization conditions. In natural conditions where temperature fluctuates widely over both daily and seasonal cycles or in different *FLC* alleles (16) that have different silencing dynamics, the quantitative contributions of processes reducing *FLC* transcription, including *COOLAIR*, may differ.

A surprising finding from this study that needs to be pursued is the high stability of the *FLC* mRNA. It may be physiologically important in natural conditions because any reduction in temperature could immediately influence *FLC* transcription. High stability of *FLC* mRNA could buffer fluctuating temperatures, avoiding large changes in *FLC* activity that would precipitate precocious flowering. The RNA stability may also play an important role in the time averaging mechanisms the plant must use to monitor the weeks and months required for full vernalization. Our knowledge is limited about how environmental inputs are integrated with epigenetic-modification pathways to regulate stress or adaptation responses. Deciphering chromatin modifications events, their interactions, and dynamics on *FLC* is providing a paradigm for environmental epigenetic regulation generally.

Materials and Methods

Plant Material, Growth Conditions, and Cold Treatment. Seeds were sown on GM-glucose media plates and stratified for 2 d. For nonvernalized samples, seedlings were grown in long-day conditions for 10 d (16-h light at 20 °C, 8-h darkness at 16 °C). For vernalization, seeds were pregrown for 10 d at standard warm growing conditions (16-h light at 20 °C, 8-h darkness at 16 °C) before being transferred to cold (8-h light and 16-h darkness at 5 °C) for 2 wk, and then returned to warm conditions for 7 d.

Terminator Exchange Lines. Generation of *TEX* lines has been fully described in ref. 10. We used the mixed samples from approximately 50 individual transgenic lines, Basta-resistant T3 generation heterozygote/homozygote mix, to analyze RNA expression in both *CTL* (named as CTLp) and *TEX* constructs (named as TEXp), (method has been described in ref. 16). One homozygous T3 representative line (*TEX577*, here renamed as *TEX1*) was chosen to generate the *vrn5-5/TEX1* genotype (9). Similarly, we randomly selected one homozygous T3 transgenic line from the *CTL* pool (CTL).

Chromatin Immunoprecipitation. ChIP experiments were done as described (6), using anti-H3 (Abcam; ab1791), anti-H3K27me3 (Millipore; 07-449), and anti-H3K36me3 (Abcam; ab9050). The ChIP data were quantified by quantitative PCR, normalizing to internal reference genes. *STM* (At1g62360) was used as the reference gene for H3K27me3 and *ACT1N* (At5g09810) for H3K36me3.

Chromatin Isolation by RNA Purification. ChIRP was performed as described (19). A detailed protocol can be found in SI Appendix, SI Materials and Methods.

GFP Fusion Proteins and Western Blotting. The GFP-SWN line is described in ref. 21. VRN5-EYFP is described in ref. 23. Magnetic GFP-Trap beads (ChromoTek) were used for pull-down YFP tagged VRN5 and SWN, and anti-GFP antibody (Roche) was used for the Western blot shown in SI Appendix, Fig. S8A.

ACKNOWLEDGMENTS. We thank The Sainsbury Lab (Norwich) for making the ChIRP-seq DNA library; Martin Trick for help with ChIRP-seq data analysis; Scott Berry for helping to plot Fig. 1D; Andrew Angel for analysis of tiling array data and plotting SI Appendix, Fig. S4; and Timothy Wells for the assistant of plant growth. Discussion with all C.D. laboratory members is much appreciated. This work is supported by a UK Biotechnology and Biological Sciences Research Council Institute Strategic Programme Grant BB/J004588/1 to John Innes Centre, and a European Research Council Advanced Investigator grant (ENVGENE) (to C.D.).

1. Michaels SD, Amasino RM (1999) FLOWERING LOCUS C encodes a novel MADS domain protein that acts as a repressor of flowering. *Plant Cell* 11(5):949–956.
2. Sheldon CC, Rouse DT, Finnegan EJ, Peacock WJ, Dennis ES (2000) The molecular basis of vernalization: The central role of FLOWERING LOCUS C (*FLC*). *Proc Natl Acad Sci USA* 97(7):3753–3758.

3. Sheldon CC, et al. (1999) The *FLC* MADS box gene: A repressor of flowering in *Arabidopsis* regulated by vernalization and methylation. *Plant Cell* 11(3):445–458.
4. Gendall AR, Levy YY, Wilson A, Dean C (2001) The *VERNALIZATION 2* gene mediates the epigenetic regulation of vernalization in *Arabidopsis*. *Cell* 107(4):525–535.

5. De Lucia F, Crevillen P, Jones AM, Greb T, Dean C (2008) A PHD-polycomb repressive complex 2 triggers the epigenetic silencing of FLC during vernalization. *Proc Natl Acad Sci USA* 105(44):16831–16836.
6. Angel A, Song J, Dean C, Howard M (2011) A Polycomb-based switch underlying quantitative epigenetic memory. *Nature* 476(7358):105–108.
7. Yang H, Howard M, Dean C (2014) Antagonistic roles for H3K36me3 and H3K27me3 in the cold-induced epigenetic switch at Arabidopsis FLC. *Curr Biol* 24(15):1793–1797.
8. Liu F, Marquardt S, Lister C, Swiezewski S, Dean C (2010) Targeted 3' processing of antisense transcripts triggers Arabidopsis FLC chromatin silencing. *Science* 327(5961):94–97.
9. Marquardt S, et al. (2014) Functional consequences of splicing of the antisense transcript COOLAIR on FLC transcription. *Mol Cell* 54(1):156–165.
10. Wang ZW, Wu Z, Raitskin O, Sun Q, Dean C (2014) Antisense-mediated FLC transcriptional repression requires the P-TEFb transcription elongation factor. *Proc Natl Acad Sci USA* 111(20):7468–7473.
11. Swiezewski S, Liu F, Magusin A, Dean C (2009) Cold-induced silencing by long antisense transcripts of an Arabidopsis Polycomb target. *Nature* 462(7274):799–802.
12. Hornyk C, Duc C, Rataj K, Terzi LC, Simpson GG (2010) Alternative polyadenylation of antisense RNAs and flowering time control. *Biochem Soc Trans* 38(4):1077–1081.
13. Sun Q, Csorba T, Skourti-Stathaki K, Proudfoot NJ, Dean C (2013) R-loop stabilization represses antisense transcription at the Arabidopsis FLC locus. *Science* 340(6132):619–621.
14. Helliwell CA, Robertson M, Finnegan EJ, Buzas DM, Dennis ES (2011) Vernalization-repression of Arabidopsis FLC requires promoter sequences but not antisense transcripts. *PLoS ONE* 6(6):e21513.
15. Gutierrez RA, Ewing RM, Cherry JM, Green PJ (2002) Identification of unstable transcripts in Arabidopsis by cDNA microarray analysis: Rapid decay is associated with a group of touch- and specific clock-controlled genes. *Proc Natl Acad Sci USA* 99(17):11513–11518.
16. Coustham V, et al. (2012) Quantitative modulation of polycomb silencing underlies natural variation in vernalization. *Science* 337(6094):584–587.
17. Narsai R, et al. (2007) Genome-wide analysis of mRNA decay rates and their determinants in Arabidopsis thaliana. *Plant Cell* 19(11):3418–3436.
18. Batista PJ, Chang HY (2013) Long noncoding RNAs: Cellular address codes in development and disease. *Cell* 152(6):1298–1307.
19. Chu C, Qu K, Zhong FL, Artandi SE, Chang HY (2011) Genomic maps of long non-coding RNA occupancy reveal principles of RNA-chromatin interactions. *Mol Cell* 44(4):667–678.
20. Finnegan EJ, Dennis ES (2007) Vernalization-induced trimethylation of histone H3 lysine 27 at FLC is not maintained in mitotically quiescent cells. *Curr Biol* 17(22):1978–1983.
21. Wang D, Tyson MD, Jackson SS, Yadegari R (2006) Partially redundant functions of two SET-domain polycomb-group proteins in controlling initiation of seed development in Arabidopsis. *Proc Natl Acad Sci USA* 103(35):13244–13249.
22. Dodd IB, Micheelsen MA, Sneppen K, Thon G (2007) Theoretical analysis of epigenetic cell memory by nucleosome modification. *Cell* 129(4):813–822.
23. Greb T, et al. (2007) The PHD finger protein VRN5 functions in the epigenetic silencing of Arabidopsis FLC. *Curr Biol* 17(1):73–78.
24. Dong G, Ma DP, Li J (2008) The histone methyltransferase SDG8 regulates shoot branching in Arabidopsis. *Biochem Biophys Res Commun* 373(4):659–664.
25. Kim SY, et al. (2005) Establishment of the vernalization-responsive, winter-annual habit in Arabidopsis requires a putative histone H3 methyl transferase. *Plant Cell* 17(12):3301–3310.
26. Xu L, et al. (2008) Di- and tri- but not monomethylation on histone H3 lysine 36 marks active transcription of genes involved in flowering time regulation and other processes in Arabidopsis thaliana. *Mol Cell Biol* 28(4):1348–1360.
27. Yuan W, et al. (2011) H3K36 methylation antagonizes PRC2-mediated H3K27 methylation. *J Biol Chem* 286(10):7983–7989.
28. Tanaka Y, Katagiri Z, Kawahashi K, Kiousis D, Kitajima S (2007) Trithorax-group protein ASH1 methylates histone H3 lysine 36. *Gene* 397(1–2):161–168.
29. Cartagena JA, et al. (2008) The Arabidopsis SDG4 contributes to the regulation of pollen tube growth by methylation of histone H3 lysines 4 and 36 in mature pollen. *Dev Biol* 315(2):355–368.
30. Zhao Z, Yu Y, Meyer D, Wu C, Shen WH (2005) Prevention of early flowering by expression of FLOWERING LOCUS C requires methylation of histone H3 K36. *Nat Cell Biol* 7(12):1256–1260.
31. Pedersen MT, Helin K (2010) Histone demethylases in development and disease. *Trends Cell Biol* 20(11):662–671.
32. Wang KC, Chang HY (2011) Molecular mechanisms of long noncoding RNAs. *Mol Cell* 43(6):904–914.
33. Keller C, Kulasegaran-Shylini R, Shimada Y, Hotz HR, Bühler M (2013) Noncoding RNAs prevent spreading of a repressive histone mark. *Nat Struct Mol Biol* 20(8):994–1000.
34. Sheldon CC, Conn AB, Dennis ES, Peacock WJ (2002) Different regulatory regions are required for the vernalization-induced repression of FLOWERING LOCUS C and for the epigenetic maintenance of repression. *Plant Cell* 14(10):2527–2537.
35. Seeley KA, Byrne DH, Colbert JT (1992) Red light-independent instability of oat phytochrome mRNA in vivo. *Plant Cell* 4(1):29–38.